Electron. Mater. Lett., Vol. 11, No. 6 (2015), pp. 1066-1071
DOI: 10.1007/s13391-015-4420-7

Study of Ethanolamine Surface Treatment on the Metal-Oxide Electron Transport Layer in Inverted InP Quantum Dot Light-Emitting Diodes

Ilwan Jang,[1,2,†] Jiwan Kim,[2,†] Chang Jun Park,[1] Christian Ippen,[3] Tonino Greco,[3] Min Suk Oh,[2] Jeongno Lee,[2] Won Keun Kim,[2] Armin Wedel,[3] Chul Jong Han,[2,*] and Sung Kyu Park[1,*]

[1]Department of Electrical and Electronics Engineering, Chung Ang University, Seoul 156-756, Korea
[2]Display Convergence Research Center, Korea Electronics Technology Institute, Seongnam 463-816, Korea
[3]Fraunhofer Institute for Applied Polymer Research, Potsdam-Golm 14476, Germany

(received date: 20 November 2014 / accepted date: 7 July 2015 / published date: 10 November 2015)

The present work shows the effect of ethanolamine surface treatment on inverted InP quantum dot light-emitting diodes (QD-LEDs) with inorganic metal oxide layers. In the inverted structure of ITO/ZnO/InP QDs/CBP/MoO_3/Al, a sol-gel derived ZnO film was used as an electron transport layer (ETL) and MoO_3 was used as a hole injection layer (HIL). First, ethanolamine was treated as a surface modifier on top of the ZnO electron transport layer. The optical performance of the QD-LED device was improved by the ethanolamine surface treatment. Second, low temperature annealing (<200°C) was performed on the ZnO sol-gel electron transport layer, followed by an investigation of the effect of the ZnO annealing temperature. The efficiency of the inverted QD-LEDs was significantly enhanced (more than 3-fold) by optimization of the ZnO annealing temperature.

Keywords: InP QDs, quantum dot light-emitting diode (QD-LED), ethanolamine, zinc oxide

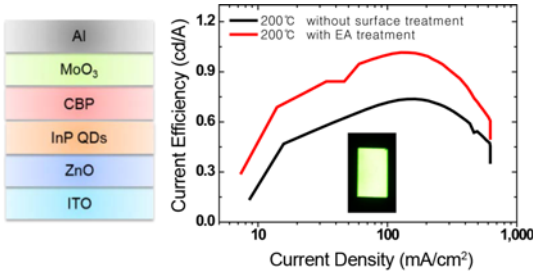

1. INTRODUCTION

Colloidal quantum-dot based light-emitting didoes (QD-LEDs) have been highly spotlighted as the next generation display due to the unique properties of colloidal quantum dots (CQDs) such as a narrow full width at half maximum (FWHM), color tunable luminescence, and cost-effective solution processability.[1-3] Since the first emergence of QD-LEDs in 1994, the great progress has been made by many research groups over two decades. Although the performance of state-of-the-art QD-LEDs is now catching up with that of organic light emitting diodes (OLEDs), most QD-LEDs are fabricated with cadmium (Cd) based CQDs such as CdSe and CdS.[2,4,5] Since Cd is a toxic element, it has necessitated research into QD-LEDs with Cd-free CQDs such as $CuInS_2$, ZnCuInS, ZnSe, and InP.[6-10] Among possible core materials of Cd-free CQDs, InP is a strong candidate due to its wide spectrum range and well-matched energy level.[9,10]

QD-LEDs with an inverted structure recently have been studied due to their promising results over conventional structures.[2,4,11] Various strategies have been investigated to improve the carrier transport at the interface between the inorganic charge transport layer and active emissive layer. In this regard, various surface modifying layers such as a self-assembled-dipole-monolayer (SADM), ionic liquid molecules (ILMs), and a polar solvent have been demonstrated to improve the charge transport and interfacial contact resistance, which results in increased device efficiency.[12,13] The inverted QD-LED with metal oxides showed better electrical/optical efficiency and stability, which is due to the robust and chemically stable properties of the inorganic charge transport

†These authors equally contributed to this work.
*Corresponding author: cjhan@keti.re.kr
*Corresponding author: skpark@cau.ac.kr

layer for solution processed QD deposition.[4,14] Additionally, the surface modification of the ZnO layer was already a proven technique, but most studies applied it only to PLED. Since the emitting materials are different (organic for PLED vs. inorganic for QD-LED), we believe that our study could be valuable and contribute to promising further research on InP-based QD-LEDs.

In this study, the temperature-dependent properties of the ZnO interlayer as well as the effect of the ethanolamine (EA) surface treatment, and their corresponding device performance were studied for better device efficiency. Previously, inverted QD-LEDs with a sol-gel derived ZnO electron transport layer (ETL) were investigated by changing the annealing time and temperature of the ZnO layer.[15] Here, more detailed analysis of ZnO interlayers such as the surface state and work function was performed for efficient charge recombination in the QD emissive layer. The performance of the inverted QD-LEDs was efficiently improved by EA surface treatment and following optimization of the ZnO annealing temperature. In the case of InP QDs based QD-LEDs, the best performance was 10.9 cd/A and 3900 cd/m^2,[16] and our results (3.5 cd/A and 3790 cd/m^2) are comparable with them.

2. EXPERIMENTAL PROCEDURE

2.1 Synthesis of InP CQDs

InP multishell QDs were synthesized by the heating-up method and the detailed synthesis procedure is described in our recent publication.[17] Briefly, InP cores were synthesized by first heating a mixture of indium(III) acetate and zinc octanoate until homogenous melting followed by adding dodecanethiol and tris(trimethylsilyl)phosphine, and subsequently heating the mixture to 300°C for 30 min. The InP core nanoparticles were capped with a ZnSe/ZnS multishell by adding trioctylphosphine selenide and heating to 280°C for 20 min. Subsequently, a ZnS outer shell was grown in two steps by adding further zinc and a sulfur precursor and heating to 280°C for 10 min. The raw solution of multishell QDs was purified several times and then it was redispersed in nonane for fabrication of the QD-LED device.

2.2 Fabrication of QD-LEDs

First, the ITO glass patterned for a cathode was cleaned by sonication using sequentially acetone, methanol and isopropyl alcohol (IPA). The cleaned ITO cathode was dried and O_2 plasma was treated on the surface of the ITO film for 5 min. Then, the sol-gel derived ZnO solution was made for the ETL. 0.1812 g of zinc acetate dihydrate [$Zn(C_4H_6O_4)\cdot 2H_2O$] was dissolved in 5 mL of 2-methoxyethanol and the concentration of ZnO was fixed to 0.165 M. This solution was stirred for 1 h at 75°C, and subsequently heated up to 200°C, and it remained for about 5 min to get a clear solution of ZnO. The purification of the ZnO solution was performed by a 0.2 μm PTFE filter. This purified solution was spin-coated on the ITO substrate at a rate of 1000 rpm for 40 s. The spin-coated substrate was placed on the 50°C hotplate to evaporate the residual solvent. The temperature of the underlying hotplate was increased up to 130, 150, 200°C, respectively (about 15 nm), to observe the effect of the annealing temperature. After that, 5 wt. % of EA diluted in 2-methoxyethanol (2-ME) was spin-coated on the ZnO layer at a rate of 3000 rpm for 20 s followed by annealing at 130°C with a hotplate for 10 min. For deposition of an emissive layer, InP/ZnSe/ZnS QDs was spin-coated at 3000 rpm for 20 s. After these solution processes, the hole transport layer (HTL) of 4,4'-N,N'-dicarbazole-biphenyl (CBP) (60 nm), HIL of MoO_3 (10 nm), and an Al (150 nm) anode were deposited sequentially by thermal evaporation. Finally, the encapsulation glass was covered to passivate the QD-LED from the ambient air containing water vapor and oxygen.

2.3 Characterization

The electroluminescence (EL) and current density-voltage-luminance (J-V-L) were measured by using a spectroradiometer (Minolta-CS 1000) with a Keithley 2400 source meter and silicon photodiode (FDS100). All the measurements were performed in the ambient condition. The luminance and current efficiency were measured by the photodiode and then correctly calibrated with the luminance value captured by a spectroradiometer CS-1000. The surface profiles of the ZnO layer were measured by atomic force microscopy (AFM). The work functions of the ZnO layers were carefully measured using ultraviolet photoelectron spectroscopy (PHI 5000 VersaProbe) under ultra-high vacuum condition (10^{-9} Torr).

3. RESULTS AND DISCUSSION

InP/ZnSe/ZnS quantum dots were synthesized with a convenient heating-up method. The heating-up synthesis is simple and reproducible compared with the hot-injection method due to the removal of the manual injection process. The detailed material properties such as the photoluminescence (PL) spectra and transmission electron microscopy images are described in our recent publication.[17] Briefly, the particle size was about 2.5 nm and the PL showed improvement by adding an outer shell and the small red-shift by the formation of the outer shell.

Figure 1 shows the schematic structure of the inverted QD-LEDs. The device structure is composed of ITO glass as a cathode/sol-gel derived ZnO as an ETL/InP based multishell QDs as an emissive layer/CBP as a HTL/MoO_3 as a HIL/Al as an anode. By using the inverted structure, in contrast to the conventional structure, electrons and holes are injected

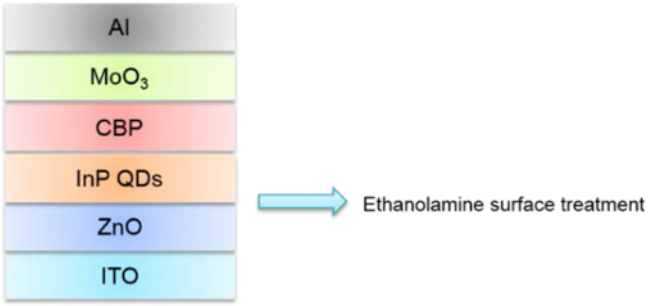

Fig. 1. Cross-sectional structure of inverted InP QD-LEDs.

into the InP QDs through the ZnO sol-gel film (ETL) and CBP (HTL) from ITO (cathode) and Al (anode), respectively. In this inverted structure, the underlying ZnO ETL can efficiently facilitate electron injection from the ITO cathode and also block the holes.[18]

Since organic charge transport materials in the OLED devices can be easily influenced by oxygen and water,[12] the robust metal oxides (ZnO and MoO_3) provide several advantages for the charge transport layers of the inverted QD-LEDs. The underlying ZnO is optically transparent in the visible region and suitable for optoelectronic devices. It also provides a robust mechanical platform for the solution-process deposition of InP QDs. Due to the relatively low crystallization temperature and easy composition controllability,[19,20] the sol-gel method was adopted for deposition of the ZnO layer. In optoelectronic devices with an inverted structure such as QD-LEDs and solar cells, the EA surface treatment on top of the ZnO ETL was performed to obtain better surface morphology and device efficiency.[13,14] For the first step of the optimization, ethanolamine was treated on top of the ZnO ETL to improve the interface between ETL and the QDs emissive layer. The effect of the ethanolamine surface treatment was investigated by comparing two QD-LED devices with a 200°C annealed ZnO layer. Secondly, the effect of the annealing temperature of ZnO ETL was investigated by measuring the electrical and optical properties of the QD-LEDs.

Figure 2 shows the electrical and optical characteristics of QD-LEDs at the 200°C annealing temperature of the ZnO layer without and with surface treatment. The improvement in the optical properties is much bigger than that of the electrical properties. In Fig. 2(a), the leakage current was almost the same after the EA surface treatment. The luminance and current efficiency was increased with EA treatment in Figs. 2(b) and 2(c). The optical properties of the inverted QD-LEDs reached a peak of 3790 cd/m^2 and 1.015 cd/A when the EA treatment was performed on the ZnO layer.

Figure 3 shows the electrical/optical characteristics of QD-LEDs with EA surface treatment at the three different

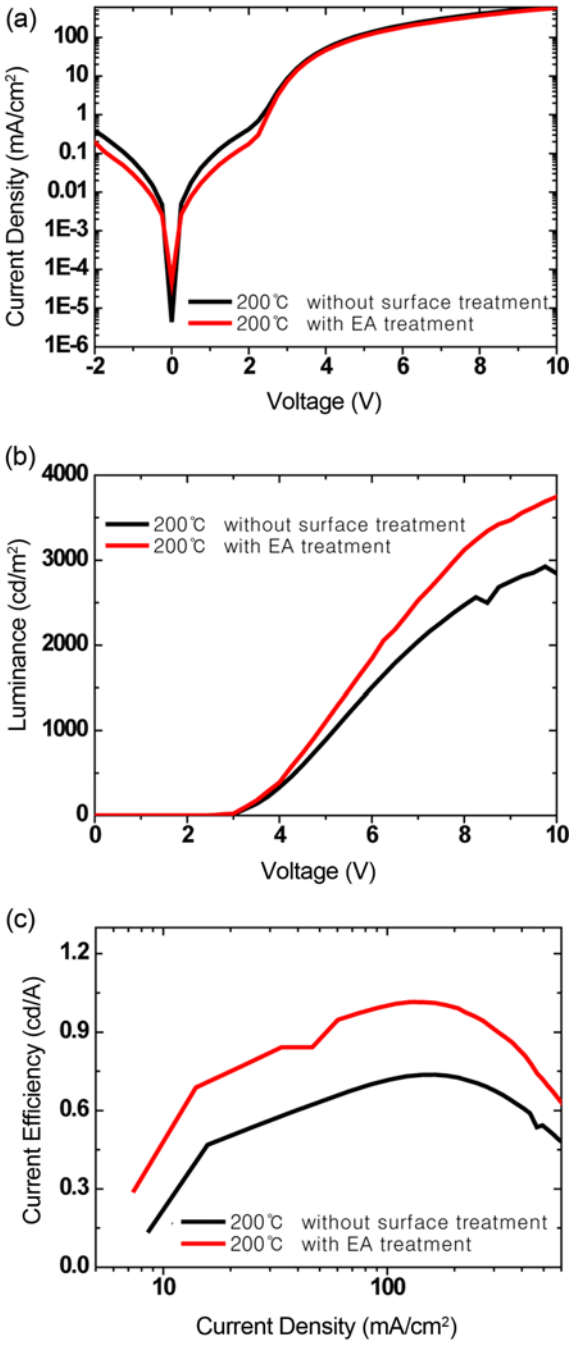

Fig. 2. (a) Current density-voltage, (b) luminance-voltage, and (c) current efficiency-voltage of inverted QD-LEDs at 200°C annealing temperatures of the ZnO layer without and with surface treatment.

annealing temperatures of the ZnO ETL. The leakage current was significantly reduced by lowering the annealing temperature in Fig. 3(a). The current efficiency was also efficiently improved more than 3 times (from 1.015 to 3.473 cd/A), when compared with the 200 and 130°C annealing temperature in Fig. 3(c).

Figure 4 shows the normalized EL spectra of the EA

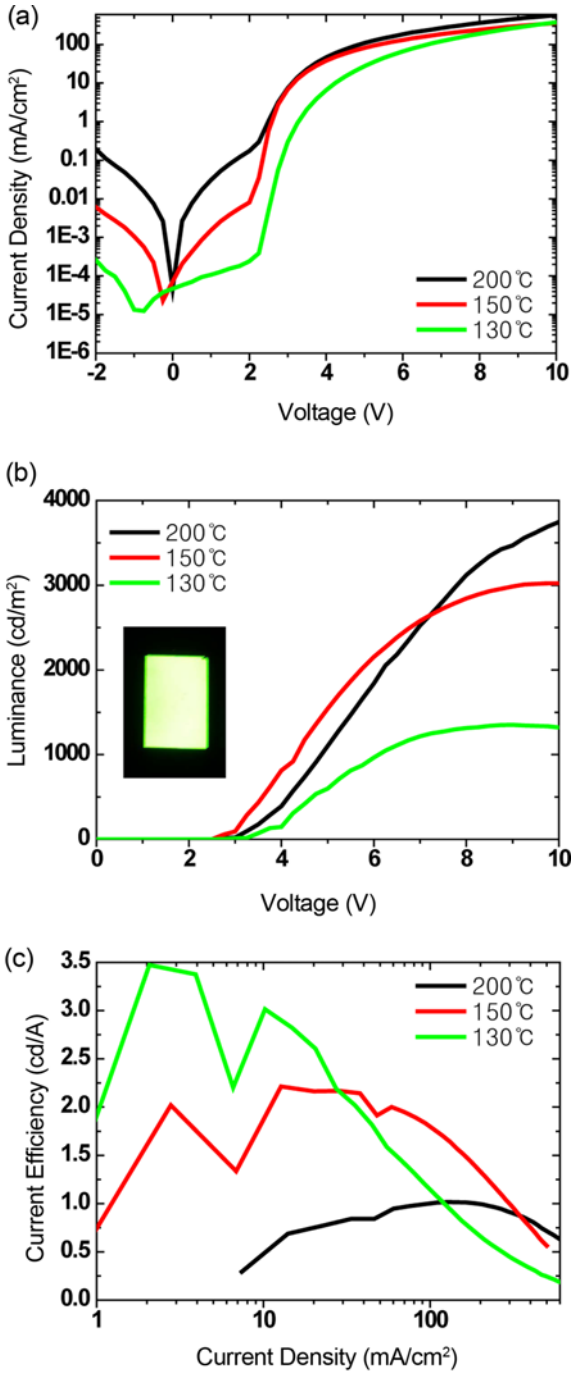

Fig. 3. (a) Current density-voltage, (b) luminance-voltage, and (c) current efficiency-current density of QD-LEDs at three different annealing temperatures (200, 150, and 130°C) of the ZnO layer with EA surface treatment. The inset of (b) shows the EL emission of a device annealed at 130°C with EA surface treatment at a constant current of 3 mA (274.5 cd/m^2).

surface treated QD-LEDs according to the annealing temperature. As shown in Fig. 4, a small parasitic emission from the CBP at 400 nm was shown in the device with ZnO

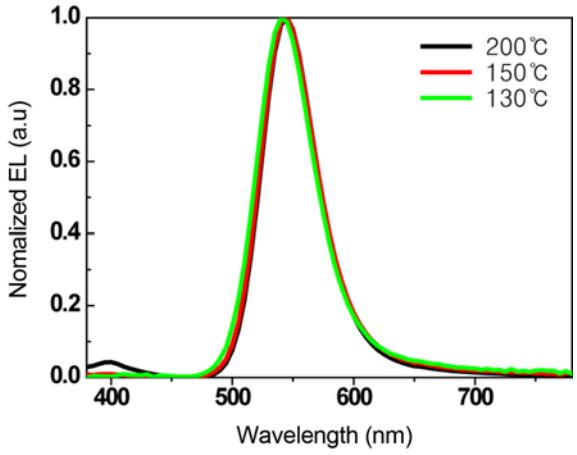

Fig. 4. The normalized EL spectra of QD-LEDs with different annealing temperatures.

annealed at 200°C. The parasitic CBP emission disappeared when the annealing temperature (150 and 130°C) was lowered. It is widely known that the mobility of ZnO made by the sol-gel method is proportional to the annealing temperature.[18,21] The reduced electron mobility triggered the transfer of the electron-hole recombination zone to the InP QDs emissive layer from the CBP-InP QDs interface, which leads to the decreased parasitic CBP emission.

The surface profiles of the ZnO films were measured by AFM to observe the surface roughness according to the EA surface treatment and the annealing temperature (200, 150 and 130°C). Figurs 5(a) and 5(b) show the AFM images of the ZnO layers at 130°C annealing without and with EA surface treatment. Figure 5(c) shows the AFM results (surface roughness) of the ZnO films according to the temperature and EA treatment. In the case of the EA treated ZnO layer at 200 and 150°C, the results of our previous report were used.[15] It is remarkable that the rms roughness of ZnO was decreased at all annealing temperatures after the EA treatment. After the EA surface treatment, the InP emissive layer was coated more uniformly on the ZnO ETL and the number of pin-holes of the QD emissive layer can be decreased with the EA coating. Additionally, electrons from the ITO cathode can be impeded by the relatively high energy barrier (>1 eV) between the LUMO of the ZnO ETL and InP QDs. Since the EA surface treatment can modify the work function of the ZnO sol-gel,[12,13] the charge carrier transport can be more easily facilitated and thus the enhanced luminance and current efficiency were obtained as shown in Figs. 2(b) and 2(c).

As shown in Fig. 5(c) and 5(d), both surface roughness and work function were slightly increased at a higher annealing temperature. The increased roughness was due to the fact that the grain size of ZnO sol-gel is proportional to the annealing temperature. As a result of the EA surface

(a)

(b)

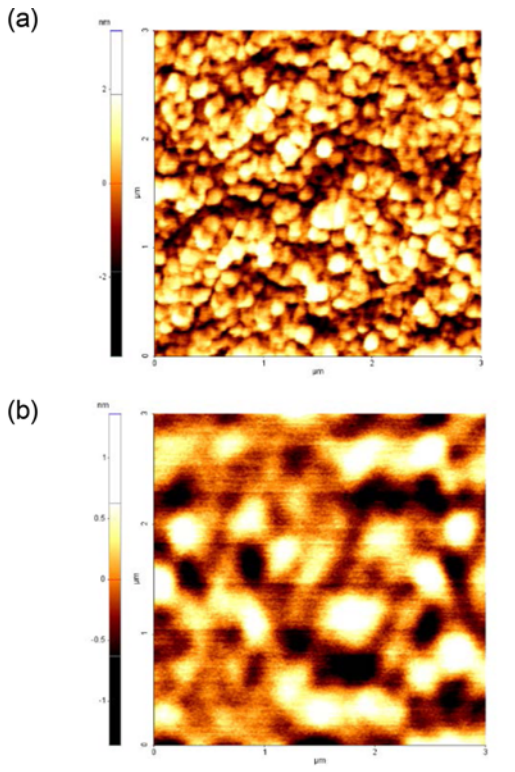

(c)

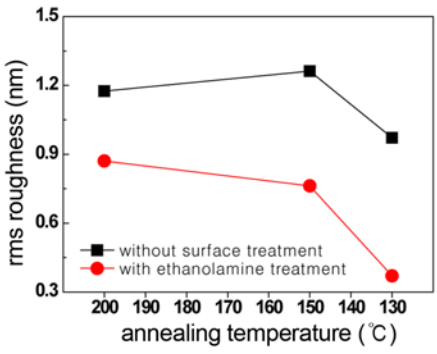

(d)

Annealing temperature	130℃	150℃	200℃
Roughness (nm)	0.370	0.762	0.871
Work function (eV)	3.4	4.3	4.5

Fig. 5. AFM images of the ZnO layer at 130°C annealing (a) without and (b) with EA treatment, respectively. (c) Results of AFM measurements (rms roughness) at three different annealing temperatures (200, 150 and 130°C) according to the surface treatment.[15] (d) Characteristics of ZnO films with different annealing temperatures.

treatment of the ZnO ETL and the optimized annealing temperature, the number of the electron carrier population became more balanced at the QDs emissive layer, which in turn shows the improvement of efficiency in QD-LEDs. The inverted QD-LED with ZnO ETL annealed at 130°C shows the best result (3.5 cd/A), and has the smoothest surface and also helps make an efficient charge balance at the emission layer.

4. CONCLUSIONS

QD-LEDs with an inverted structure were fabricated using Cd-free InP based QDs. Inorganic charge transport layers such as ZnO sol-gel and MoO_3 were used as an ETL and HIL, respectively. For the surface modification, an ethanolamine solution was spin-coated on top of the ZnO ETL. The surface roughness of the ZnO layers was reduced and the luminance and efficiency of the QD-LEDs were efficiently improved by EA surface treatment. The effect of the annealing temperature of the ZnO layer on the characteristics of the QD-LEDs was investigated to improve the optimization of the QD-LED devices. Under the optimal condition of 130°C annealing, the current efficiency was significantly enhanced from 1.015 to 3.473 cd/A. The results of the AFM measurement showed that the more uniform ZnO layer was formed as decreasing the ZnO annealing temperature. It is noteworthy that a small parasitic emission from the CBP layer was completely eliminated. It is attributed to the reduced ZnO electron mobility of the lower annealing temperature, which promotes the shift of the electron-hole recombination zone from the CBP-InP QDs interface to the InP QDs. The results of the optimization of the sol-gel derived ZnO ETL and EA surface treatment demonstrated the efficiently improved performance of the inverted InP QD-LEDs.

ACKOWLEDGEMENTS

This work was supported by Dual Use Technology Program funded by the Civil Military Technology Cooperation Center (CMTC, Korea) and Chung-Ang University Excellent Student Scholarship in 2014.

REFERENCES

1. S. Coe, W. Woo, M. Bawendi, and V. Bulović, *Nature* **420**, 800 (2002).
2. B. S. Mashford, M. Stevenson, Z. Popovic, C. Hamilton, Z. Zhou, C. Breen, J. Steckel, V. Bulović, M. Bawendi, S. Coe, and P. T. Kazlas, *Nat. Photonics* **7**, 407 (2013).
3. R. Khan, J. W. Jeon, L. W. Jang, M. K. Kim, E. Y. Ko, J. I. Lee, and I. H. Lee, *Electron. Mater. Lett.* **10**, 451 (2014).
4. L. Qian, Y. Zheng, J. Xue, and P. H. Holloway, *Nat. Photonics* **5**, 543 (2011).
5. J. Kwak, W. K. Bae, D. Lee, I. Park, J. Lim, M. Park, H. Cho, H. Woo, D. Y. Yoon, K. Char, S. Lee, and C. Lee, *Nano Lett.* **12**, 2362 (2012).
6. Z. Tan, Y. Zhang, C. Xie, H. Su, J. Liu, C. Zhang, N.

Dellas, S. E. Mohney, Y. Wang, J. Wang, and J. Xu, *Adv. Mater.* **23**, 3553 (2011).
7. W. Ji, P. Jing, W. Xu, X. Yuan, Y. Wang, J. Zhao, and A. Jen, *Appl. Phys. Lett*. **103**, 053106 (2013).
8. M. Taherian, A. A. Sabbagh Alvani, M. A. Shokrgozar, R. Salimi, S. Moosakhani, H. Sameie, and F. Tabatabaee, *Electron. Mater. Lett.* **10**, 393 (2014).
9. C. Ippen, T. Greco, and A. Wedel, *J. Inf. Disp*. **13**, 91 (2012).
10. X. Yang, D. Zhao, K. S. Leck, S. T. Tan, Y. X. Tang, J. Zhao, H. V. Demir, and X. W. Sun, *Adv. Mater.* **24**, 4180 (2012).
11. H. Kim, A. Yusoff, J. Youn, and J. Jang, *J. Mater. Chem. C* **1**, 3924 (2013).
12. B. Lee, E. Jung, Y. Nam, M. Jung, J. Park, S. Lee, H. Choi, S. Ko, N. Shin, Y. Kim, S. Kim, J. Kim, H. Shin, S. Cho, and M. Song, *Adv. Mater.* **26**, 494 (2014).
13. B. Lee, E. Jung, J. Park, Y. Nam, S. Min, B. Kim, K. Lee, J. Jeong, R. H. Friend, J. Kim, S. Kim, and M. Song, *Nat. Commun.* **5**, 4840 (2014).
14. K. Cho, E. K. Lee, W. Joo, E. Jang, T. Kim, S. J. Lee, S. Kwon, J. Y. Han, B. Kim, B. L. Choi, and J. M. Kim, *Nat. Photonics* **3**, 341 (2009).
15. I. Jang, J. Kim, C. Ippen, T. Greco, M. S. Oh, J. Lee, W. K. Kim, A. Wedel, C. J. Han, and S. K. Park, *Jpn. J. Appl. Phys.* **54**, 02BC01 (2015).
16. J. Lim, M. Park, W. K. Bae, D. Lee, S. Lee, C. Lee, and K. Char, *ACS Nano* **7**, 9019 (2013).
17. Y. Kim, C. Ippen, T. Greco, J. Lee, M. S. Oh, C. J. Han, A. Wedel, and J. Kim, *Opt. Mater. Express* **4**, 1436 (2014).
18. Y. Sun, J. H. Seo, C. J. Takacs, J. Seifter, and A. J. Heeger, *Adv. Mater.* **23**, 1679 (2011).
19. T. Ivanova, A. Harizanova, T. Koutzarova, and B. Vertruyen, *Mater. Lett.* **64**, 1147 (2010).
20. S. O'Brien, L. H. K. Koh, and G. M. Crean, *Thin Solid Films* **516**, 1391 (2008).
21. J. Lee, K. Ko, and B. Park, *J. Cryst. Growth* **247**, 119 (2003).